Cosmological Signal Processing

Jason McEwen

http://www.jasonmcewen.org/

Department of Physics and Astronomy
University College London (UCL)

University of Southampton :: October 2012

Outline

Outline

1. Cosmology
   - Cosmological concordance model
   - Cosmological observations
2. Wavelet on the sphere
   - Euclidean wavelets
   - Continuous wavelets on the sphere
   - Scale-discretised wavelets on the sphere
3. Cosmic strings
   - Observational signatures
   - Estimating the string tension
   - Recovering string maps
4. Wavelets on the ball
   - Scale-discretised wavelets on the ball
5. Compressive sensing
   - An introduction to compressive sensing
6. Radio interferometry
   - Interferometric imaging
   - Sparsity averaging reweighted analysis (SARA)
   - Future

Cosmological concordance model

- Concordance model of modern cosmology emerged recently with many cosmological parameters constrained to high precision.
- General description is of a Universe undergoing accelerated expansion, containing 4% ordinary baryonic matter, 22% cold dark matter and 74% dark energy.
- Structure and evolution of the Universe constrained through cosmological observations.

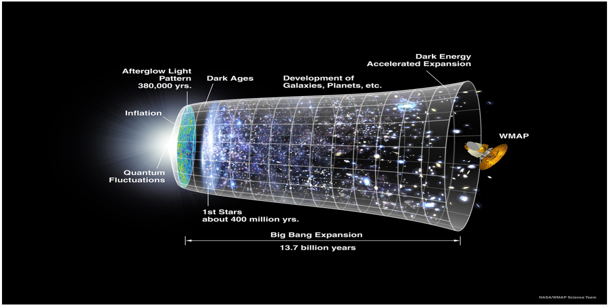

[Credit: WMAP Science Team]

Observations of the cosmic microwave background (CMB)

- Full-sky observations of the cosmic microwave background (CMB).

(a) COBE (launched 1989)

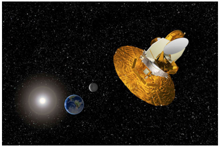

(b) WMAP (launched 2001)

(c) Planck (launched 2009)

- Each new experiment provides dramatic improvement in precision and resolution of observations.

(cobe 2 wmap movie)

(planck movie)

(d) COBE to WMAP [Credit: WMAP Science Team]

(e) Planck observing strategy [Credit: Planck Collaboration]

Cosmic microwave background (CMB)

- Observations of the CMB made by WMAP have played a large role in constraining the cosmological concordance model.

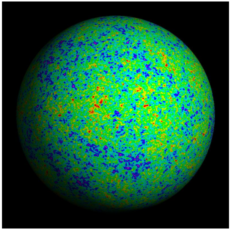

(a) Temperature anisotropies

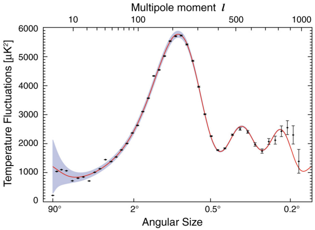

(b) Power spectrum

Figure: CMB observations [Credit: WMAP Science Team]

- Although a general cosmological concordance model is now established, many details remain unclear. Study of well-motivated extensions of the cosmological concordance model now important.
- CMB observed on spherical manifold, hence the geometry of the sphere must be taken into account in any analysis.

Outline

Why wavelets?

Fourier (1807)

Haar (1909)

Morlet and Grossman (1981)

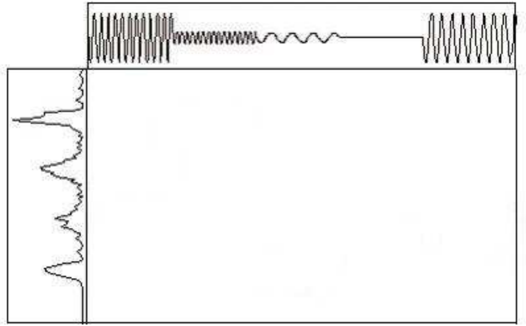

Figure: Fourier vs wavelet transform (credit: http://www.wavelet.org/tutorial/)

Why wavelets?

Fourier (1807)

Haar (1909)

Morlet and Grossman (1981)

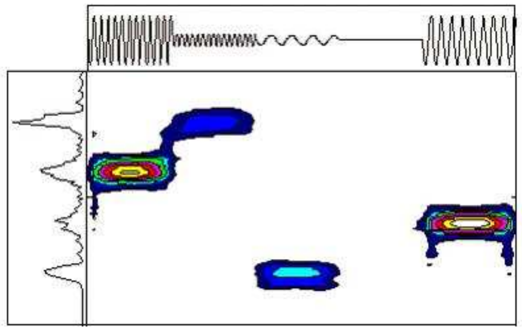

Figure: Fourier vs wavelet transform (credit: `http://www.wavelet.org/tutorial/`)

Wavelet transform in Euclidean space

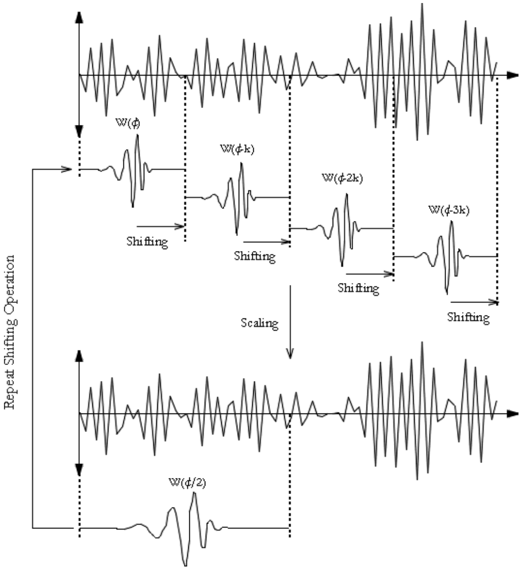

Figure: Wavelet scaling and shifting (image from `http://www.wavelet.org/tutorial/`)

Continuous wavelets on the sphere

- First natural wavelet construction on the sphere was derived in the seminal work of Antoine and Vandergheynst (1998) (reintroduced by Wiaux 2005).
- Construct wavelet atoms from affine transformations (dilation, translation) on the sphere of a mother wavelet.
- The natural extension of translations to the sphere are rotations. Rotation of a function f on the sphere is defined by

$$[\mathcal{R}(\rho)f](\omega) = f(\rho^{-1}\omega), \quad \omega = (\theta, \varphi) \in \mathrm{S}^2, \quad \rho = (\alpha, \beta, \gamma) \in \mathrm{SO}(3) \ .$$

- How define dilation on the sphere?
- The spherical dilation operator is defined through the conjugation of the Euclidean dilation and stereographic projection Π:

$$\mathcal{D}(a) \equiv \Pi^{-1}\, d(a)\, \Pi \ .$$

Continuous wavelets on the sphere

- First natural wavelet construction on the sphere was derived in the seminal work of Antoine and Vandergheynst (1998) (reintroduced by Wiaux 2005).
- Construct wavelet atoms from affine transformations (dilation, translation) on the sphere of a mother wavelet.
- The natural extension of translations to the sphere are rotations. Rotation of a function f on the sphere is defined by

$$[\mathcal{R}(\rho)f](\omega) = f(\rho^{-1}\omega), \quad \omega = (\theta, \varphi) \in \mathrm{S}^2, \quad \rho = (\alpha, \beta, \gamma) \in \mathrm{SO}(3) \; .$$

- How define dilation on the sphere?
- The spherical dilation operator is defined through the conjugation of the Euclidean dilation and stereographic projection Π:

$$\mathcal{D}(a) \equiv \Pi^{-1} \, d(a) \, \Pi \; .$$

Continuous wavelets on the sphere

- First natural wavelet construction on the sphere was derived in the seminal work of Antoine and Vandergheynst (1998) (reintroduced by Wiaux 2005).
- Construct wavelet atoms from affine transformations (dilation, translation) on the sphere of a mother wavelet.
- The natural extension of translations to the sphere are rotations. Rotation of a function f on the sphere is defined by

$$[\mathcal{R}(\rho) f](\omega) = f(\rho^{-1}\omega), \quad \omega = (\theta, \varphi) \in \mathrm{S}^2, \quad \rho = (\alpha, \beta, \gamma) \in \mathrm{SO}(3) .$$

- How define dilation on the sphere?
- The spherical dilation operator is defined through the conjugation of the Euclidean dilation and stereographic projection Π:

$$\mathcal{D}(a) \equiv \Pi^{-1}\, d(a)\, \Pi .$$

Continuous wavelets on the sphere

- First natural wavelet construction on the sphere was derived in the seminal work of Antoine and Vandergheynst (1998) (reintroduced by Wiaux 2005).
- Construct wavelet atoms from affine transformations (dilation, translation) on the sphere of a mother wavelet.
- The natural extension of translations to the sphere are rotations. Rotation of a function f on the sphere is defined by

$$[\mathcal{R}(\rho)f](\omega) = f(\rho^{-1}\omega), \quad \omega = (\theta, \varphi) \in \mathrm{S}^2, \quad \rho = (\alpha, \beta, \gamma) \in \mathrm{SO}(3) \ .$$

- How define dilation on the sphere?
- The spherical dilation operator is defined through the conjugation of the Euclidean dilation and stereographic projection Π:

$$\mathcal{D}(a) \equiv \Pi^{-1}\, d(a)\, \Pi \ .$$

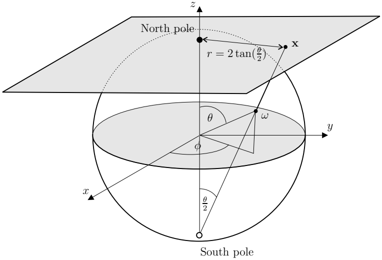

Figure: Stereographic projection.

Continuous wavelet analysis

- Wavelet frame on the sphere constructed from rotations and dilations of a mother spherical wavelet Φ:

$$\{\Phi_{a,\rho} \equiv \mathcal{R}(\rho)\mathcal{D}(a)\Phi \,:\, \rho \in \mathrm{SO}(3),\, a \in \mathbb{R}_*^+\}.$$

- The forward wavelet transform is given by

$$\boxed{W_\Phi^f(a,\rho) = \langle f, \Phi_{a,\rho}\rangle = \int_{\mathrm{S}^2} \mathrm{d}\Omega(\omega)\, f(\omega)\, \Phi_{a,\rho}^*(\omega)\,,}$$

where $\mathrm{d}\Omega(\omega) = \sin\theta\,\mathrm{d}\theta\,\mathrm{d}\varphi$ is the usual invariant measure on the sphere.

- Transform general in the sense that all orientations in the rotation group $\mathrm{SO}(3)$ are considered, thus directional structure is naturally incorporated.

- Fast algorithms essential (for a review see Wiaux, JDM & Vielva 2007)
  - Factoring of rotations: JDM *et al.* (2007), Wandelt & Gorski (2001)
  - Separation of variables: Wiaux *et al.* (2005)

- FastCSWT code available to download: http://www.jasonmcewen.org/

Continuous wavelet analysis

- Wavelet frame on the sphere constructed from rotations and dilations of a mother spherical wavelet Φ:

$$\{\Phi_{a,\rho} \equiv \mathcal{R}(\rho)\mathcal{D}(a)\Phi : \rho \in \mathrm{SO}(3),\, a \in \mathbb{R}_*^+\}.$$

- The forward wavelet transform is given by

$$\boxed{W_\Phi^f(a,\rho) = \langle f, \Phi_{a,\rho}\rangle = \int_{\mathrm{S}^2} \mathrm{d}\Omega(\omega)\, f(\omega)\, \Phi_{a,\rho}^*(\omega)\ ,}$$

where $\mathrm{d}\Omega(\omega) = \sin\theta \,\mathrm{d}\theta\, \mathrm{d}\varphi$ is the usual invariant measure on the sphere.

- Transform general in the sense that all orientations in the rotation group $\mathrm{SO}(3)$ are considered, thus directional structure is naturally incorporated.

- Fast algorithms essential (for a review see Wiaux, JDM & Vielva 2007)
  - Factoring of rotations: JDM *et al.* (2007), Wandelt & Gorski (2001)
  - Separation of variables: Wiaux *et al.* (2005)

- FastCSWT code available to download: http://www.jasonmcewen.org/

Continuous wavelet analysis

- Wavelet frame on the sphere constructed from rotations and dilations of a mother spherical wavelet Φ:

$$\{\Phi_{a,\rho} \equiv \mathcal{R}(\rho)\mathcal{D}(a)\Phi : \rho \in \mathrm{SO}(3),\, a \in \mathbb{R}_*^+\}.$$

- The forward wavelet transform is given by

$$\boxed{W_\Phi^f(a,\rho) = \langle f, \Phi_{a,\rho}\rangle = \int_{\mathrm{S}^2} \mathrm{d}\Omega(\omega)\, f(\omega)\, \Phi_{a,\rho}^*(\omega)\ ,}$$

  where $\mathrm{d}\Omega(\omega) = \sin\theta\, \mathrm{d}\theta\, \mathrm{d}\varphi$ is the usual invariant measure on the sphere.

- Transform general in the sense that all orientations in the rotation group $\mathrm{SO}(3)$ are considered, thus directional structure is naturally incorporated.

- Fast algorithms essential (for a review see Wiaux, JDM & Vielva 2007)
  - Factoring of rotations: JDM *et al.* (2007), Wandelt & Gorski (2001)
  - Separation of variables: Wiaux *et al.* (2005)

- FastCSWT code available to download: `http://www.jasonmcewen.org/`

Mother wavelets

- Correspondence principle between spherical and Euclidean wavelets states that the inverse stereographic projection of an *admissible* wavelet on the plane yields an *admissible* wavelet on the sphere (proved by Wiaux *et al.* 2005)
- Mother wavelets on sphere constructed from the projection of mother Euclidean wavelets defined on the plane:

$$\Phi = \Pi^{-1}\Phi_{\mathbb{R}^2} ,$$

where $\Phi_{\mathbb{R}^2} \in L^2(\mathbb{R}^2, d^2\boldsymbol{x})$ is an admissible wavelet in the plane.
- Directional wavelets on sphere may be naturally constructed in this setting – they are simply the projection of directional Euclidean planar wavelets on to the sphere.

Mother wavelets

- Correspondence principle between spherical and Euclidean wavelets states that the inverse stereographic projection of an *admissible* wavelet on the plane yields an *admissible* wavelet on the sphere (proved by Wiaux *et al.* 2005)
- Mother wavelets on sphere constructed from the projection of mother Euclidean wavelets defined on the plane:

$$\Phi = \Pi^{-1}\Phi_{\mathbb{R}^2} \; ,$$

  where $\Phi_{\mathbb{R}^2} \in \mathrm{L}^2(\mathbb{R}^2, \, \mathrm{d}^2\boldsymbol{x})$ is an admissible wavelet in the plane.
- Directional wavelets on sphere may be naturally constructed in this setting – they are simply the projection of directional Euclidean planar wavelets on to the sphere.

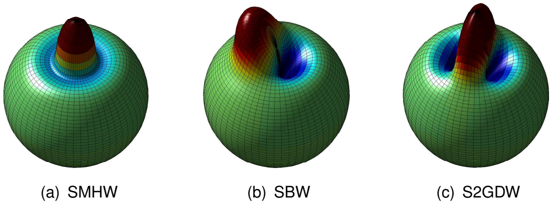

Figure: Spherical wavelets at scale $a, b = 0.2$.

Continuous wavelet synthesis (reconstruction)

- The inverse wavelet transform given by

$$\boxed{f(\omega) = \int_0^\infty \frac{\mathrm{d}a}{a^3} \int_{\mathrm{SO}(3)} \mathrm{d}\varrho(\rho) W_\Phi^f(a,\rho)\, [\mathcal{R}(\rho)\widehat{L}_\Phi \Phi_a](\omega)\ ,}$$

where $\mathrm{d}\varrho(\rho) = \sin\beta\, \mathrm{d}\alpha\, \mathrm{d}\beta\, \mathrm{d}\gamma$ is the invariant measure on the rotation group $\mathrm{SO}(3)$.

- Perfect reconstruction is ensured provided wavelets satisfy the admissibility property:

$$\boxed{0 < \widehat{C}_\Phi^\ell \equiv \frac{8\pi^2}{2\ell+1} \sum_{m=-\ell}^{\ell} \int_0^\infty \frac{\mathrm{d}a}{a^3} \mid (\Phi_a)_{\ell m} \mid^2 < \infty, \quad \forall \ell \in \mathbb{N}}$$

where $(\Phi_a)_{\ell m}$ are the spherical harmonic coefficients of $\Phi_a(\omega)$.

- Continuous wavelets used effectively in many cosmological studies, for example:
  - Non-Gaussianity (*e.g.* Vielva *et al.* 2004; JDM *et al.* 2005, 2006, 2008)
  - ISW (*e.g.* Vielva *et al.* 2005, JDM *et al.* 2007, 2008)

- BUT...

Continuous wavelet synthesis (reconstruction)

- The inverse wavelet transform given by

$$\boxed{f(\omega) = \int_0^\infty \frac{\mathrm{d}a}{a^3} \int_{\mathrm{SO}(3)} \mathrm{d}\varrho(\rho) W_\Phi^f(a, \rho) \, [\mathcal{R}(\rho) \widehat{L}_\Phi \Phi_a](\omega) \ ,}$$

  where $\mathrm{d}\varrho(\rho) = \sin\beta \, \mathrm{d}\alpha \, \mathrm{d}\beta \, \mathrm{d}\gamma$ is the invariant measure on the rotation group $\mathrm{SO}(3)$.

- Perfect reconstruction is ensured provided wavelets satisfy the admissibility property:

$$\boxed{0 < \widehat{C}_\Phi^\ell \equiv \frac{8\pi^2}{2\ell+1} \sum_{m=-\ell}^{\ell} \int_0^\infty \frac{\mathrm{d}a}{a^3} \mid (\Phi_a)_{\ell m} \mid^2 < \infty, \quad \forall \ell \in \mathbb{N}}$$

  where $(\Phi_a)_{\ell m}$ are the spherical harmonic coefficients of $\Phi_a(\omega)$.

- Continuous wavelets used effectively in many cosmological studies, for example:
  - Non-Gaussianity (*e.g.* Vielva *et al.* 2004; JDM *et al.* 2005, 2006, 2008)
  - ISW (*e.g.* Vielva *et al.* 2005, JDM *et al.* 2007, 2008)

- BUT...

Continuous wavelet synthesis (reconstruction)

- The inverse wavelet transform given by

$$\boxed{f(\omega) = \int_0^\infty \frac{\mathrm{d}a}{a^3} \int_{\mathrm{SO}(3)} \mathrm{d}\varrho(\rho) W^f_\Phi(a,\rho)\,[\mathcal{R}(\rho)\widehat{L}_\Phi \Phi_a](\omega)\ ,}$$

where $\mathrm{d}\varrho(\rho) = \sin\beta\,\mathrm{d}\alpha\,\mathrm{d}\beta\,\mathrm{d}\gamma$ is the invariant measure on the rotation group $\mathrm{SO}(3)$.

- Perfect reconstruction is ensured provided wavelets satisfy the admissibility property:

$$\boxed{0 < \widehat{C}^\ell_\Phi \equiv \frac{8\pi^2}{2\ell+1} \sum_{m=-\ell}^{\ell} \int_0^\infty \frac{\mathrm{d}a}{a^3} \mid (\Phi_a)_{\ell m} \mid^2 < \infty, \quad \forall \ell \in \mathbb{N}}$$

where $(\Phi_a)_{\ell m}$ are the spherical harmonic coefficients of $\Phi_a(\omega)$.

- Continuous wavelets used effectively in many cosmological studies, for example:
  - Non-Gaussianity (*e.g.* Vielva *et al.* 2004; JDM *et al.* 2005, 2006, 2008)
  - ISW (*e.g.* Vielva *et al.* 2005, JDM *et al.* 2007, 2008)

- BUT... **exact reconstruction not feasible in practice!**

Scale-discretised wavelets on the sphere

- Wiaux, JDM, Vandergheynst, Blanc (2008)
  Exact reconstruction with directional wavelets on the sphere
  S2DW code

- Dilation performed in harmonic space.
  Following JDM *et al.* (2006), Sanz *et al.* (2006).

- The scale-discretised wavelet $\Psi \in L^2(S^2, d\Omega)$ is defined in harmonic space:

$$\widehat{\Psi}_{\ell m} = \tilde{K}_\Psi(\ell) S^\Psi_{\ell m} \, .$$

- Construct wavelets to satisfy a resolution of the identity for $0 \leq \ell < L$:

$$\tilde{\Phi}^2_\Psi(\alpha^J \ell) + \sum_{j=0}^{J} \tilde{K}^2_\Psi(\alpha^j \ell) = 1 \, .$$

Scale-discretised wavelets on the sphere

- Wiaux, JDM, Vandergheynst, Blanc (2008)
  Exact reconstruction with directional wavelets on the sphere
  S2DW code

- Dilation performed in harmonic space.
  Following JDM *et al.* (2006), Sanz *et al.* (2006).

- The scale-discretised wavelet $\Psi \in \mathrm{L}^2(\mathrm{S}^2, \mathrm{d}\Omega)$ is defined in harmonic space:

$$\widehat{\Psi}_{\ell m} = \tilde{K}_\Psi(\ell) S^\Psi_{\ell m} \, .$$

- Construct wavelets to satisfy a resolution of the identity for $0 \leq \ell < L$:

$$\tilde{\Phi}^2_\Psi(\alpha^J \ell) + \sum_{j=0}^{J} \tilde{K}^2_\Psi(\alpha^j \ell) = 1 \, .$$

Scale-discretised wavelets on the sphere

- Wiaux, JDM, Vandergheynst, Blanc (2008)
  Exact reconstruction with directional wavelets on the sphere
  S2DW code

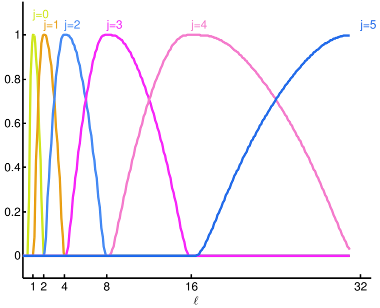

Figure: Harmonic tiling on the sphere.

- Dilation performed in harmonic space.
  Following JDM *et al.* (2006), Sanz *et al.* (2006).

- The scale-discretised wavelet $\Psi \in \mathrm{L}^2(\mathrm{S}^2, \mathrm{d}\Omega)$ is defined in harmonic space:

$$\widehat{\Psi}_{\ell m} = \tilde{K}_\Psi(\ell) S^\Psi_{\ell m} \ .$$

- Construct wavelets to satisfy a resolution of the identity for $0 \leq \ell < L$:

$$\tilde{\Phi}^2_\Psi(\alpha^J \ell) + \sum_{j=0}^{J} \tilde{K}^2_\Psi(\alpha^j \ell) = 1 .$$

Scale-discretised wavelets

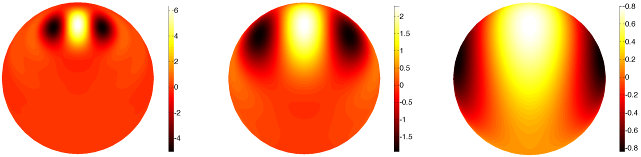

Figure: Spherical scale-discretised wavelets.

- The scale-discretised wavelet transform is given by the usual projection onto each wavelet:

$$\boxed{W_{\Psi}^{f}(\rho, \alpha^{j}) = \langle f, \Psi_{\rho, \alpha^{j}} \rangle = \int_{S^2} \mathrm{d}\Omega(\omega)\, f(\omega)\, \Psi_{\rho, \alpha^{j}}^{*}(\omega)\,.}$$

- The original function may be recovered exactly in practice from the wavelet (and scaling) coefficients:

$$\boxed{f(\omega) = \left[\Phi_{\alpha^{J}} f\right](\omega) + \sum_{j=0}^{J} \int_{\mathrm{SO}(3)} \mathrm{d}\varrho(\rho)\, W_{\Psi}^{f}\left(\rho, \alpha^{j}\right) \left[R(\rho)\, L^{\mathrm{d}} \Psi_{\alpha^{j}}\right](\omega)\,.}$$

Scale-discretised wavelets

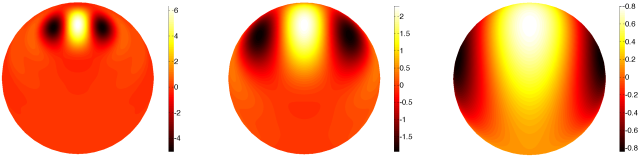

Figure: Spherical scale-discretised wavelets.

- The scale-discretised wavelet transform is given by the usual projection onto each wavelet:

$$\boxed{W^f_\Psi(\rho, \alpha^j) = \langle f, \Psi_{\rho,\alpha^j} \rangle = \int_{S^2} d\Omega(\omega)\, f(\omega)\, \Psi^*_{\rho,\alpha^j}(\omega)\ .}$$

- The original function may be recovered exactly in practice from the wavelet (and scaling) coefficients:

$$\boxed{f(\omega) = [\Phi_{\alpha^J} f](\omega) + \sum_{j=0}^{J} \int_{SO(3)} d\varrho(\rho)\, W^f_\Psi\left(\rho, \alpha^j\right) \left[R(\rho)\, L^d \Psi_{\alpha^j}\right](\omega)\ .}$$

Scale-discretised wavelets

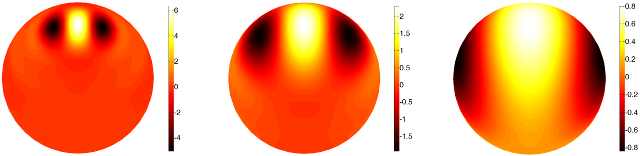

Figure: Spherical scale-discretised wavelets.

- The scale-discretised wavelet transform is given by the usual projection onto each wavelet:

$$\boxed{W^f_\Psi(\rho, \alpha^j) = \langle f, \Psi_{\rho,\alpha^j} \rangle = \int_{S^2} \mathrm{d}\Omega(\omega)\, f(\omega)\, \Psi^*_{\rho,\alpha^j}(\omega)\ .}$$

- The original function may be recovered exactly in practice from the wavelet (and scaling) coefficients:

$$\boxed{f(\omega) = [\Phi_{\alpha^J} f](\omega) + \sum_{j=0}^{J} \int_{\mathrm{SO}(3)} \mathrm{d}\varrho(\rho)\, W^f_\Psi\left(\rho, \alpha^j\right) \left[R(\rho)\, L^{\mathrm{d}} \Psi_{\alpha^j}\right](\omega)\ .}$$

Scale-discretised wavelet transform of the Earth

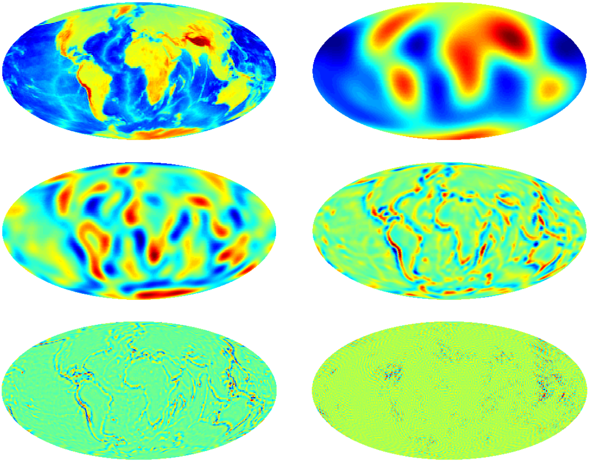

Figure: Scale-discretised wavelet transform of a topography map of the Earth.

Codes for scale-discretised wavelets on the sphere

S2DW code

Exact reconstruction with directional wavelets on the sphere
Wiaux, JDM, Vandergheynst, Blanc (2008)

- Fortran
- Supports directional, steerable wavelets

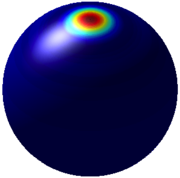

S2LET code

S2LET: A code to perform fast wavelet analysis on the sphere
Leistedt, JDM, Wiaux, Vandergheynst (2012)

- C, Matlab, IDL, Java
- Support only axisymmetric wavelets at present
- Future extensions:
  - Directional, steerable wavelets
  - Faster algorithms to perform wavelet transforms
  - Spin wavelets

All codes available from: `http://www.jasonmcewen.org/`

Outline

Cosmic strings

- Symmetry breaking phase transitions in the early Universe → topological defects.
- Cosmic strings well-motivated phenomenon that arise when axial or cylindrical symmetry is broken → line-like discontinuities in the fabric of the Universe.
- Although we have not yet observed cosmic strings, we have observed string-like topological defects in other media, e.g. ice and liquid crystal.
- Cosmic strings are distinct to the fundamental superstrings of string theory.
- However, recent developments in string theory suggest the existence of macroscopic superstrings that could play a similar role to cosmic strings.
- **The detection of cosmic strings would open a new window into the physics of the Universe!**

Figure: Optical microscope photograph of a thin film of freely suspended nematic liquid crystal after a temperature quench. [Credit: Chuang *et al.* (1991).]

Cosmic strings

- Symmetry breaking phase transitions in the early Universe → topological defects.
- Cosmic strings well-motivated phenomenon that arise when axial or cylindrical symmetry is broken → line-like discontinuities in the fabric of the Universe.
- Although we have not yet observed cosmic strings, we have observed string-like topological defects in other media, e.g. ice and liquid crystal.
- Cosmic strings are distinct to the fundamental superstrings of string theory.
- However, recent developments in string theory suggest the existence of macroscopic superstrings that could play a similar role to cosmic strings.
- The detection of cosmic strings would open a new window into the physics of the Universe!

Figure: Optical microscope photograph of a thin film of freely suspended nematic liquid crystal after a temperature quench. [Credit: Chuang *et al.* (1991).]

Cosmic strings

- Symmetry breaking phase transitions in the early Universe $\rightarrow$ topological defects.
- Cosmic strings well-motivated phenomenon that arise when axial or cylindrical symmetry is broken $\rightarrow$ line-like discontinuities in the fabric of the Universe.
- Although we have not yet observed cosmic strings, we have observed string-like topological defects in other media, e.g. ice and liquid crystal.
- Cosmic strings are distinct to the fundamental superstrings of string theory.
- However, recent developments in string theory suggest the existence of macroscopic superstrings that could play a similar role to cosmic strings.
- **The detection of cosmic strings would open a new window into the physics of the Universe!**

Figure: Optical microscope photograph of a thin film of freely suspended nematic liquid crystal after a temperature quench. [Credit: Chuang *et al.* (1991).]

Observational signatures of cosmic strings

- Spacetime about a cosmic string is canonical, with a three-dimensional wedge removed (Vilenkin 1981).
- Strings moving transverse to the line of sight induce line-like discontinuities in the CMB (Kaiser & Stebbins 1984).
- The amplitude of the induced contribution scales with $G\mu$, the string tension.

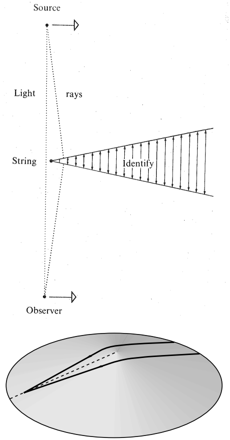

Figure: Spacetime around a cosmic string.
[Credit: Kaiser & Stebbins 1984, DAMTP.]

Observational signatures of cosmic strings

- Make contact between theory and data using high-resolution simulations.
- High-resolution full-sky simulations created by Christophe Ringeval.

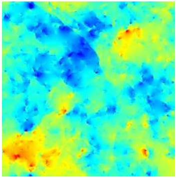

(a) Flat patch (Fraisse *et al.* 2008)

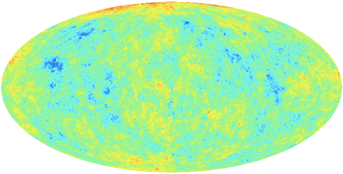

(b) Full-sky (Ringeval *et al.* 2012)

Figure: Cosmic string simulations.

Observational signatures of cosmic strings

- Make contact between theory and data using high-resolution simulations.
- High-resolution full-sky simulations created by Christophe Ringeval.

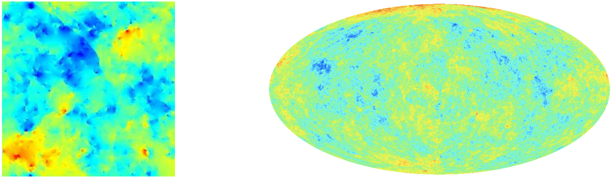

(a) Flat patch (Fraisse *et al.* 2008) (b) Full-sky (Ringeval *et al.* 2012)

Figure: Cosmic string simulations.

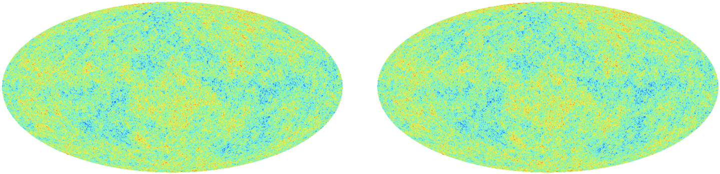

(a) CMB (b) CMB with embedded string

Figure: CMB simulation with string contribution ($G\mu = 5 \times 10^{-7}$) embedded .

Motivation for using wavelets to detect cosmic strings

- Adopt the scale-discretised wavelet transform on the sphere (Wiaux, JDM *et al.* 2008), where we denote the wavelet coefficients of the data d by $\boxed{W^d_{j\rho} = \langle d,\ \Psi_{j\rho} \rangle}$ for scale $j \in \mathbb{Z}^+$ and position $\rho \in \mathrm{SO}(3)$.
- Consider an even azimuthal band-limit $N = 4$ to yield wavelet with odd azimuthal symmetry.

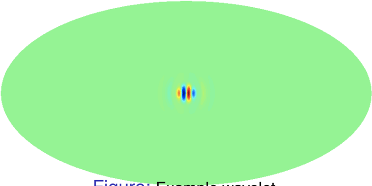

Figure: Example wavelet.

- Wavelet transform yields a sparse representation of the string signal $\rightarrow$ hope to effectively separate the CMB and string signal in wavelet space.

Motivation for using wavelets to detect cosmic strings

- Adopt the scale-discretised wavelet transform on the sphere (Wiaux, JDM *et al.* 2008), where we denote the wavelet coefficients of the data d by $\boxed{W^d_{j\rho} = \langle d,\ \Psi_{j\rho} \rangle}$ for scale $j \in \mathbb{Z}^+$ and position $\rho \in \mathrm{SO}(3)$.
- Consider an even azimuthal band-limit $N = 4$ to yield wavelet with odd azimuthal symmetry.

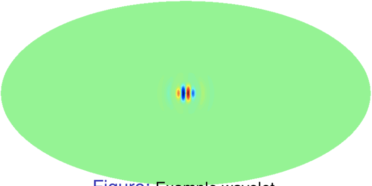

Figure: Example wavelet.

- Wavelet transform yields a sparse representation of the string signal $\rightarrow$ hope to effectively separate the CMB and string signal in wavelet space.

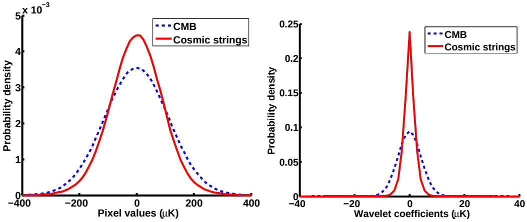

Figure: Distribution of CMB and string signal in pixel (left) and wavelet space (right).

Learning the statistics of the CMB and string signals in wavelet space

- Need to determine statistical description of the CMB and string signals in wavelet space.
- Calculate analytically the probability distribution of the CMB in wavelet space:

$$\mathrm{P}_j^c(W_{j\rho}^c) = \frac{1}{\sqrt{2\pi(\sigma_j^c)^2}} \, \mathrm{e}^{\left(-\frac{1}{2}\left(\frac{W_{j\rho}^c}{\sigma_j^c}\right)^2\right)} , \quad \text{where} \quad (\sigma_j^c)^2 = \langle W_{j\rho}^c \, W_{j\rho}^{c\;*} \rangle = \sum_{\ell m} C_\ell \, |(\Psi_j)_{\ell m}|^2 \, .$$

- Fit a generalised Gaussian distribution (GGD) for the wavelet coefficients of a string training map (*cf.* Wiaux *et al.* 2009):

$$\mathrm{P}_j^s(W_{j\rho}^s \mid G\mu) = \frac{\upsilon_j}{2G\mu\nu_j\Gamma(\upsilon_j^{-1})} \, \mathrm{e}^{\left(-\left|\frac{W_{j\rho}^s}{G\mu\nu_j}\right|^{\upsilon_j}\right)} ,$$

with scale parameter ν_j and shape parameter υ_j.

Learning the statistics of the CMB and string signals in wavelet space

- Need to determine statistical description of the CMB and string signals in wavelet space.
- Calculate analytically the probability distribution of the CMB in wavelet space:

$$\mathrm{P}_j^c(W_{j\rho}^c) = \frac{1}{\sqrt{2\pi(\sigma_j^c)^2}}\, \mathrm{e}^{\left(-\frac{1}{2}\left(\frac{W_{j\rho}^c}{\sigma_j^c}\right)^2\right)}, \quad \text{where} \quad (\sigma_j^c)^2 = \langle W_{j\rho}^c\, W_{j\rho}^{c\;*}\rangle = \sum_{\ell m} C_\ell \,|(\Psi_j)_{\ell m}|^2 .$$

- Fit a generalised Gaussian distribution (GGD) for the wavelet coefficients of a string training map (*cf.* Wiaux *et al.* 2009):

$$\mathrm{P}_j^s(W_{j\rho}^s \mid G\mu) = \frac{\upsilon_j}{2G\mu\nu_j\Gamma(\upsilon_j^{-1})}\, \mathrm{e}^{\left(-\left|\frac{W_{j\rho}^s}{G\mu\nu_j}\right|^{\upsilon_j}\right)},$$

with scale parameter ν_j and shape parameter υ_j.

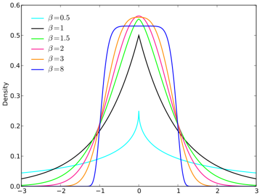

Figure: Generalised Gaussian distribution (GGD).

Learning the statistics of the CMB and string signals in wavelet space

- Require two simulated string maps: one for training; one for testing.

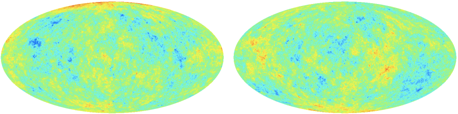

(a) String1 (b) String2

Figure: Cosmic string simulations.

- Compare distribution learnt from the training simulation (string2) with the distribution of the testing simulation (string1).
- Distributions in close agreement.

Learning the statistics of the CMB and string signals in wavelet space

- Require two simulated string maps: one for training; one for testing.

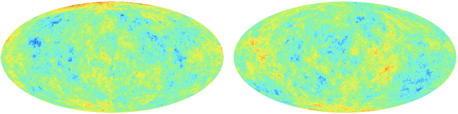

(a) String1 (b) String2

Figure: Cosmic string simulations.

- Compare distribution learnt from the training simulation (string2) with the distribution of the testing simulation (string1).
- Distributions in close agreement.

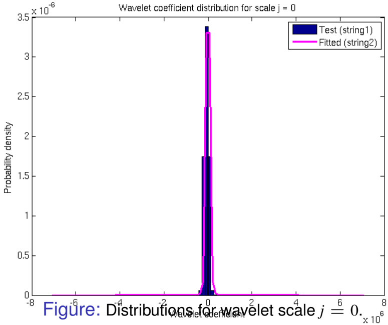

Figure: Distributions for wavelet scale $j = 0$.

Learning the statistics of the CMB and string signals in wavelet space

- Require two simulated string maps: one for training; one for testing.

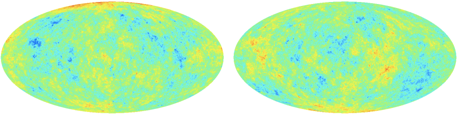

(a) String1 (b) String2

Figure: Cosmic string simulations.

- Compare distribution learnt from the training simulation (string2) with the distribution of the testing simulation (string1).
- Distributions in close agreement.

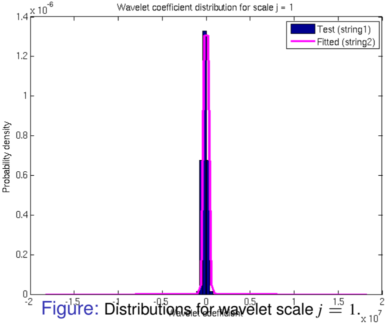

Figure: Distributions for wavelet scale $j = 1$.

Learning the statistics of the CMB and string signals in wavelet space

- Require two simulated string maps: one for training; one for testing.

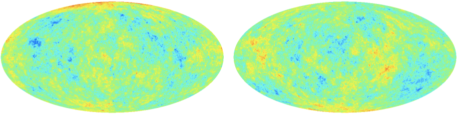

(a) String1 (b) String2

Figure: Cosmic string simulations.

- Compare distribution learnt from the training simulation (string2) with the distribution of the testing simulation (string1).
- Distributions in close agreement.

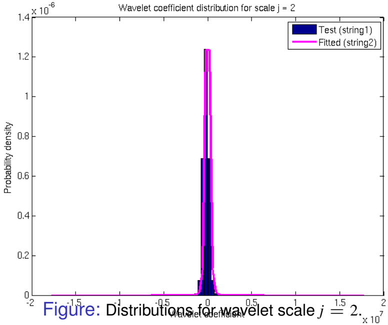

Figure: Distributions for wavelet scale $j = 2$.

Learning the statistics of the CMB and string signals in wavelet space

- Require two simulated string maps: one for training; one for testing.

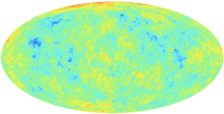

(a) String1

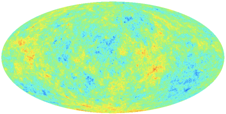

(b) String2

Figure: Cosmic string simulations.

- Compare distribution learnt from the training simulation (string2) with the distribution of the testing simulation (string1).
- Distributions in close agreement.

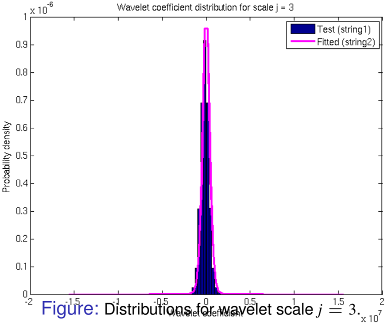

Figure: Distributions for wavelet scale $j = 3$.

Learning the statistics of the CMB and string signals in wavelet space

- Require two simulated string maps: one for training; one for testing.

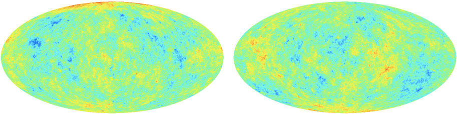

(a) String1 (b) String2

Figure: Cosmic string simulations.

- Compare distribution learnt from the training simulation (string2) with the distribution of the testing simulation (string1).
- Distributions in close agreement.

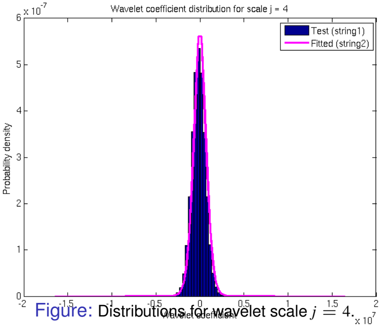

Figure: Distributions for wavelet scale $j = 4$.

Learning the statistics of the CMB and string signals in wavelet space

- Require two simulated string maps: one for training; one for testing.

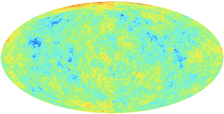

(a) String1

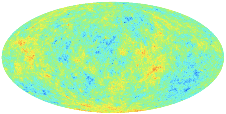

(b) String2

Figure: Cosmic string simulations.

- Compare distribution learnt from the training simulation (string2) with the distribution of the testing simulation (string1).
- Distributions in close agreement.
- We have accurately characterised the statistics of string signals in wavelet space.

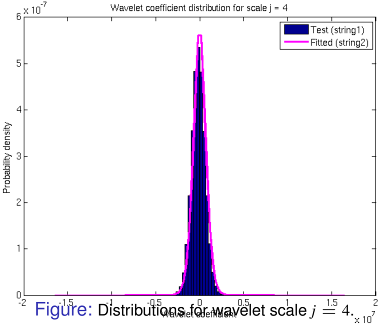

Figure: Distributions for wavelet scale $j = 4$.

Spherical wavelet-Bayesian string tension estimation

- We take a Bayesian approach to string tension estimation.
- Perform Bayesian string tension estimation in wavelet space, where the CMB and string distributions are very different.
- For each wavelet coefficient the likelihood is given by

$$\mathrm{P}(W^d_{j\rho} \mid G\mu) = \mathrm{P}(W^s_{j\rho} + W^c_{j\rho} \mid G\mu) = \int_{\mathbb{R}} \mathrm{d}W^s_{j\rho}\, \mathrm{P}^c_j(W^d_{j\rho} - W^s_{j\rho})\, \mathrm{P}^s_j(W^s_{j\rho} \mid G\mu) \,.$$

- The overall likelihood of the data is given by

$$\mathrm{P}(W^d \mid G\mu) = \prod_{j,\rho} \mathrm{P}(W^d_{j\rho} \mid G\mu) \,,$$

  where we have assumed each wavelet coefficient is independent.
- The wavelet coefficients are not independent but to incorporate the covariance of wavelet coefficients would be computationally infeasible.
- Instead, we compute the correlation length of wavelet coefficients, and only fold into the likelihood calculation wavelet coefficients that are at least a correlation length apart.
- Empirically we have found this approach to work well.

Spherical wavelet-Bayesian string tension estimation

- We take a Bayesian approach to string tension estimation.
- Perform Bayesian string tension estimation in wavelet space, where the CMB and string distributions are very different.
- For each wavelet coefficient the likelihood is given by

$$\mathrm{P}(W^d_{j\rho} \mid G\mu) = \mathrm{P}(W^s_{j\rho} + W^c_{j\rho} \mid G\mu) = \int_{\mathbb{R}} \mathrm{d}W^s_{j\rho}\, \mathrm{P}^c_j(W^d_{j\rho} - W^s_{j\rho})\, \mathrm{P}^s_j(W^s_{j\rho} \mid G\mu)\ .$$

- The overall likelihood of the data is given by

$$\mathrm{P}(W^d \mid G\mu) = \prod_{j,\rho} \mathrm{P}(W^d_{j\rho} \mid G\mu)\ ,$$

where we have assumed each wavelet coefficient is independent.

- The wavelet coefficients are not independent but to incorporate the covariance of wavelet coefficients would be computationally infeasible.
- Instead, we compute the correlation length of wavelet coefficients, and only fold into the likelihood calculation wavelet coefficients that are at least a correlation length apart.
- Empirically we have found this approach to work well.

Spherical wavelet-Bayesian string tension estimation

- We take a Bayesian approach to string tension estimation.
- Perform Bayesian string tension estimation in wavelet space, where the CMB and string distributions are very different.
- For each wavelet coefficient the likelihood is given by

$$\mathrm{P}(W^d_{j\rho} \mid G\mu) = \mathrm{P}(W^s_{j\rho} + W^c_{j\rho} \mid G\mu) = \int_{\mathbb{R}} \mathrm{d}W^s_{j\rho}\, \mathrm{P}^c_j(W^d_{j\rho} - W^s_{j\rho})\, \mathrm{P}^s_j(W^s_{j\rho} \mid G\mu)\ .$$

- The overall likelihood of the data is given by

$$\mathrm{P}(W^d \mid G\mu) = \prod_{j,\rho} \mathrm{P}(W^d_{j\rho} \mid G\mu)\ ,$$

  where we have assumed each wavelet coefficient is independent.
- The wavelet coefficients are not independent but to incorporate the covariance of wavelet coefficients would be computationally infeasible.
- Instead, we compute the correlation length of wavelet coefficients, and only fold into the likelihood calculation wavelet coefficients that are at least a correlation length apart.
- Empirically we have found this approach to work well.

Spherical wavelet-Bayesian string tension estimation

- We compute the string tension posterior $\mathrm{P}(G\mu \mid W^d)$ by Bayes theorem:

$$\mathrm{P}(G\mu \mid W^d) = \frac{\mathrm{P}(W^d \mid G\mu)\,\mathrm{P}(G\mu)}{\mathrm{P}(W^d)} \propto \mathrm{P}(W^d \mid G\mu)\,\mathrm{P}(G\mu)\ .$$

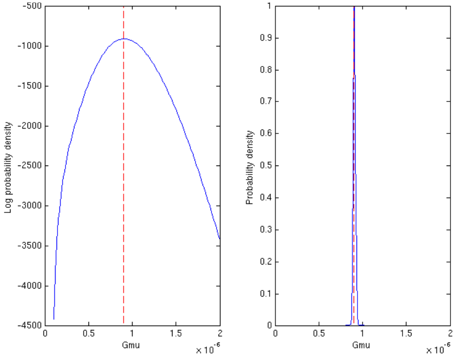

Figure: Posterior distribution of the string tension (true $G\mu = 9 \times 10^{-7}$).

Spherical wavelet-Bayesian string tension estimation

- We compute the string tension posterior $\mathrm{P}(G\mu \mid W^d)$ by Bayes theorem:

$$\mathrm{P}(G\mu \mid W^d) = \frac{\mathrm{P}(W^d \mid G\mu)\,\mathrm{P}(G\mu)}{\mathrm{P}(W^d)} \propto \mathrm{P}(W^d \mid G\mu)\,\mathrm{P}(G\mu)\ .$$

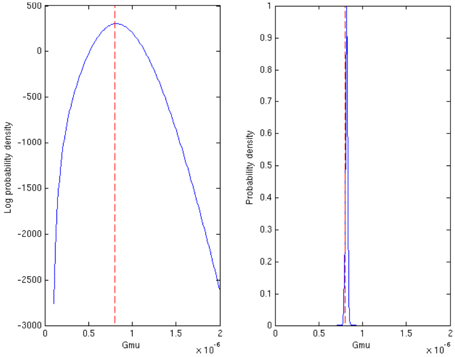

Figure: Posterior distribution of the string tension (true $G\mu = 8 \times 10^{-7}$).

Spherical wavelet-Bayesian string tension estimation

- We compute the string tension posterior $\mathrm{P}(G\mu \mid W^d)$ by Bayes theorem:

$$\mathrm{P}(G\mu \mid W^d) = \frac{\mathrm{P}(W^d \mid G\mu)\, \mathrm{P}(G\mu)}{\mathrm{P}(W^d)} \propto \mathrm{P}(W^d \mid G\mu)\, \mathrm{P}(G\mu)\ .$$

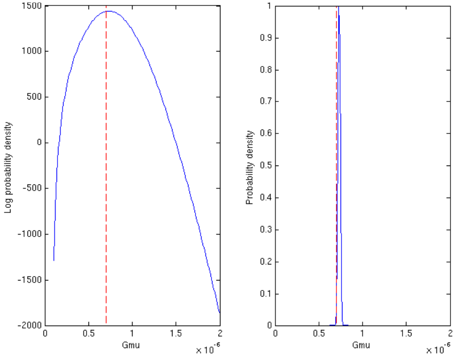

Figure: Posterior distribution of the string tension (true $G\mu = 7 \times 10^{-7}$).

Spherical wavelet-Bayesian string tension estimation

- We compute the string tension posterior $\mathrm{P}(G\mu \mid W^d)$ by Bayes theorem:

$$\mathrm{P}(G\mu \mid W^d) = \frac{\mathrm{P}(W^d \mid G\mu)\,\mathrm{P}(G\mu)}{\mathrm{P}(W^d)} \propto \mathrm{P}(W^d \mid G\mu)\,\mathrm{P}(G\mu)\ .$$

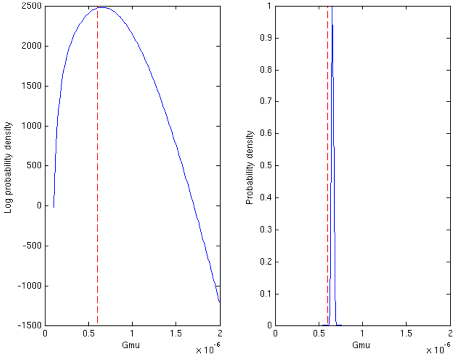

Figure: Posterior distribution of the string tension (true $G\mu = 6 \times 10^{-7}$).

Spherical wavelet-Bayesian string tension estimation

- We compute the string tension posterior $\text{P}(G\mu \mid W^d)$ by Bayes theorem:

$$\text{P}(G\mu \mid W^d) = \frac{\text{P}(W^d \mid G\mu)\, \text{P}(G\mu)}{\text{P}(W^d)} \propto \text{P}(W^d \mid G\mu)\, \text{P}(G\mu) \; .$$

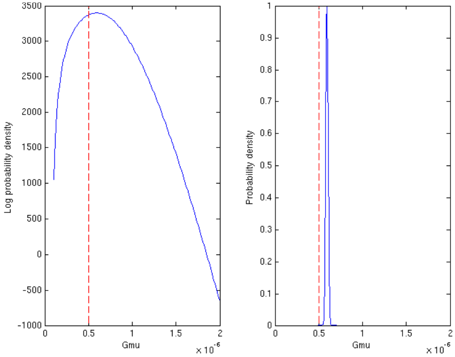

Figure: Posterior distribution of the string tension (true $G\mu = 5 \times 10^{-7}$).

Spherical wavelet-Bayesian string tension estimation

- We compute the string tension posterior $\mathrm{P}(G\mu \mid W^d)$ by Bayes theorem:

$$\mathrm{P}(G\mu \mid W^d) = \frac{\mathrm{P}(W^d \mid G\mu)\,\mathrm{P}(G\mu)}{\mathrm{P}(W^d)} \propto \mathrm{P}(W^d \mid G\mu)\,\mathrm{P}(G\mu)\ .$$

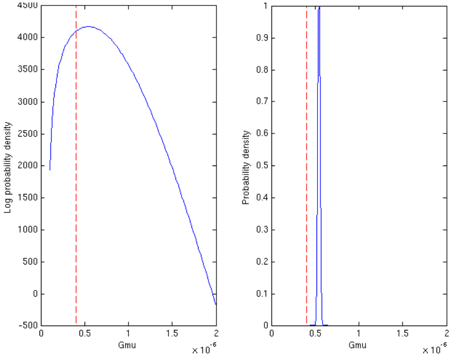

Figure: Posterior distribution of the string tension (true $G\mu = 4 \times 10^{-7}$).

Bayesian evidence for strings

- Compute Bayesian evidences to compare the string model M^s discussed so far to the alternative model M^c that the observed data is comprised of just a CMB contribution.
- The Bayesian evidence of the string model is given by

$$E^s = \mathrm{P}(W^d \mid \mathrm{M}^s) = \int_{\mathbb{R}} \mathrm{d}(G\mu)\, \mathrm{P}(W^d \mid G\mu)\, \mathrm{P}(G\mu) \,.$$

- The Bayesian evidence of the CMB model is given by

$$E^c = \mathrm{P}(W^d \mid \mathrm{M}^c) = \prod_{j,\rho} \mathrm{P}_j^c(W^d_{j\rho}) \,.$$

- Compute the Bayes factor to determine the preferred model:

$$\Delta \ln E = \ln(E^s / E^c) = \ln E^s - \ln E^c \,.$$

Bayesian evidence for strings

- Compute Bayesian evidences to compare the string model M^s discussed so far to the alternative model M^c that the observed data is comprised of just a CMB contribution.
- The Bayesian evidence of the string model is given by

$$E^s = \mathrm{P}(W^d \mid \mathrm{M}^s) = \int_{\mathbb{R}} \mathrm{d}(G\mu)\, \mathrm{P}(W^d \mid G\mu)\, \mathrm{P}(G\mu) \ .$$

- The Bayesian evidence of the CMB model is given by

$$E^c = \mathrm{P}(W^d \mid \mathrm{M}^c) = \prod_{j,\rho} \mathrm{P}_j^c(W_{j\rho}^d) \ .$$

- Compute the Bayes factor to determine the preferred model:

$$\Delta \ln E = \ln(E^s / E^c) = \ln E^s - \ln E^c \ .$$

Table: Log-evidence differences for a particular simulation.

$G\mu/10^{-7}$	2	3	4	5	6	7	8	9
$\Delta \ln E$	-278	-233	-164	-56	104	341	677	1132

Recovering string maps

- Our best inference of the wavelet coefficients of the underlying string map is encoded in the posterior probability distribution $\mathrm{P}(W^s_{j\rho} \mid W^d)$.
- Estimate the wavelet coefficients of the string map from the mean of the posterior distribution:

$$\begin{aligned}\overline{W}^s_{j\rho} &= \int_{\mathbb{R}} \mathrm{d}W^s_{j\rho}\, W^s_{j\rho}\, \mathrm{P}(W^s_{j\rho} \mid W^d) \\ &= \int_{\mathbb{R}} \mathrm{d}W^s_{j\rho}\, W^s_{j\rho} \int_{\mathbb{R}} \mathrm{d}(G\mu)\, \mathrm{P}(W^s_{j\rho} \mid W^d, G\mu)\, \mathrm{P}(G\mu \mid W^d) \\ &= \int_{\mathbb{R}} \mathrm{d}(G\mu)\, \mathrm{P}(G\mu \mid d)\, \overline{W}^s_{j\rho}(G\mu)\ ,\end{aligned}$$

  where

$$\begin{aligned}\overline{W}^s_{j\rho}(G\mu) &= \int_{\mathbb{R}} \mathrm{d}W^s_{j\rho}\, W^s_{j\rho}\, \mathrm{P}(W^s_{j\rho} \mid W^d_{j\rho}, G\mu) \\ &= \frac{1}{\mathrm{P}(W^d_{j\rho} \mid G\mu)} \int_{\mathbb{R}} \mathrm{d}W^s_{j\rho}\, W^s_{j\rho}\, \mathrm{P}^c_j(W^d_{j\rho} - W^s_{j\rho})\, \mathrm{P}^s_j(W^s_{j\rho} \mid G\mu)\ .\end{aligned}$$

- Recover the string map from its wavelets (possible since the scale-discretised wavelet transform on the sphere supports exact reconstruction).
- Work in progress...

Recovering string maps

- Our best inference of the wavelet coefficients of the underlying string map is encoded in the posterior probability distribution $\mathrm{P}(W^s_{j\rho} \mid W^d)$.
- Estimate the wavelet coefficients of the string map from the mean of the posterior distribution:

$$\begin{aligned}\overline{W}^s_{j\rho} &= \int_{\mathbb{R}} \mathrm{d}W^s_{j\rho}\; W^s_{j\rho}\; \mathrm{P}(W^s_{j\rho} \mid W^d) \\ &= \int_{\mathbb{R}} \mathrm{d}W^s_{j\rho}\; W^s_{j\rho} \int_{\mathbb{R}} \mathrm{d}(G\mu)\; \mathrm{P}(W^s_{j\rho} \mid W^d, G\mu)\; \mathrm{P}(G\mu \mid W^d) \\ &= \int_{\mathbb{R}} \mathrm{d}(G\mu)\; \mathrm{P}(G\mu \mid d)\; \overline{W}^s_{j\rho}(G\mu)\ ,\end{aligned}$$

where

$$\begin{aligned}\overline{W}^s_{j\rho}(G\mu) &= \int_{\mathbb{R}} \mathrm{d}W^s_{j\rho}\; W^s_{j\rho}\; \mathrm{P}(W^s_{j\rho} \mid W^d_{j\rho}, G\mu) \\ &= \frac{1}{\mathrm{P}(W^d_{j\rho} \mid G\mu)} \int_{\mathbb{R}} \mathrm{d}W^s_{j\rho}\; W^s_{j\rho}\; \mathrm{P}^c_j(W^d_{j\rho} - W^s_{j\rho})\; \mathrm{P}^s_j(W^s_{j\rho} \mid G\mu)\ .\end{aligned}$$

- Recover the string map from its wavelets (possible since the scale-discretised wavelet transform on the sphere supports exact reconstruction).
- Work in progress...

Recovering string maps

- Our best inference of the wavelet coefficients of the underlying string map is encoded in the posterior probability distribution $\mathrm{P}(W^s_{j\rho} \mid W^d)$.
- Estimate the wavelet coefficients of the string map from the mean of the posterior distribution:

$$\begin{aligned} \overline{W}^s_{j\rho} &= \int_{\mathbb{R}} \mathrm{d}W^s_{j\rho}\ W^s_{j\rho}\ \mathrm{P}(W^s_{j\rho} \mid W^d) \\ &= \int_{\mathbb{R}} \mathrm{d}W^s_{j\rho}\ W^s_{j\rho} \int_{\mathbb{R}} \mathrm{d}(G\mu)\ \mathrm{P}(W^s_{j\rho} \mid W^d, G\mu)\ \mathrm{P}(G\mu \mid W^d) \\ &= \int_{\mathbb{R}} \mathrm{d}(G\mu)\ \mathrm{P}(G\mu \mid d)\ \overline{W}^s_{j\rho}(G\mu)\ , \end{aligned}$$

  where

$$\begin{aligned} \overline{W}^s_{j\rho}(G\mu) &= \int_{\mathbb{R}} \mathrm{d}W^s_{j\rho}\ W^s_{j\rho}\ \mathrm{P}(W^s_{j\rho} \mid W^d_{j\rho}, G\mu) \\ &= \frac{1}{\mathrm{P}(W^d_{j\rho} \mid G\mu)} \int_{\mathbb{R}} \mathrm{d}W^s_{j\rho}\ W^s_{j\rho}\ \mathrm{P}^c_j(W^d_{j\rho} - W^s_{j\rho})\ \mathrm{P}^s_j(W^s_{j\rho} \mid G\mu)\ . \end{aligned}$$

- Recover the string map from its wavelets (possible since the scale-discretised wavelet transform on the sphere supports exact reconstruction).
- Work in progress...

Outline

Data on the ball (solid sphere)

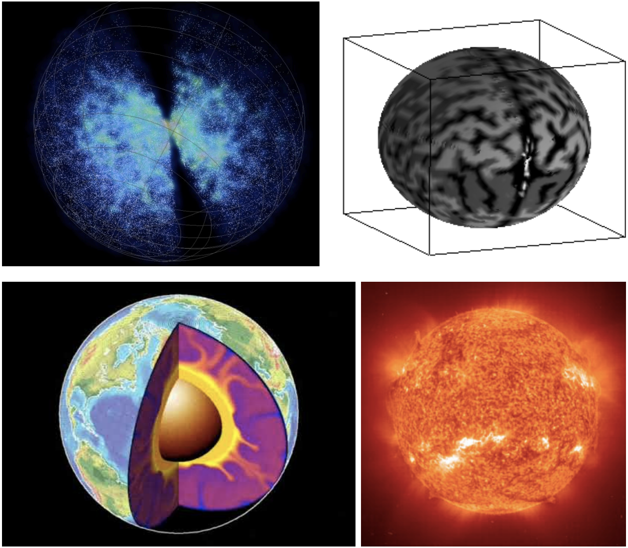

Scale-discretised wavelets on the ball

- Leistedt & JDM (2012)
  Exact wavelets on the ball
  FLAGLET code
- Define translation and convolution operator on the radial line.
- Dilation performed in harmonic space.
- The scale-discretised wavelet $\Psi \in \mathrm{L}^2(\mathrm{B}^3, \mathrm{d}^3\boldsymbol{r})$ is defined in harmonic space:

$$\Psi^{jj'}_{\ell mp} \equiv \sqrt{\frac{2\ell+1}{4\pi}}\, \kappa_\lambda\left(\frac{\ell}{\lambda^j}\right) \kappa_\nu\left(\frac{p}{\nu^{j'}}\right) \delta_{m0}\,.$$

- Construct wavelets to satisfy a resolution of the identity:

$$\frac{4\pi}{2\ell+1}\left(|\Phi_{\ell 0p}|^2 + \sum_{j=J_0}^{J}\sum_{j'=J'_0}^{J'} |\Psi^{jj'}_{\ell 0p}|^2\right) = 1, \forall \ell, p.$$

Scale-discretised wavelets on the ball

- Leistedt & JDM (2012)
  Exact wavelets on the ball
  FLAGLET code
- Define translation and convolution operator on the radial line.
- Dilation performed in harmonic space.
- The scale-discretised wavelet $\Psi \in \mathrm{L}^2(\mathrm{B}^3, \mathrm{d}^3\boldsymbol{r})$ is defined in harmonic space:

$$\Psi^{jj'}_{\ell m p} \equiv \sqrt{\frac{2\ell+1}{4\pi}}\, \kappa_\lambda\left(\frac{\ell}{\lambda^j}\right) \kappa_\nu\left(\frac{p}{\nu^{j'}}\right) \delta_{m0}.$$

- Construct wavelets to satisfy a resolution of the identity:

$$\frac{4\pi}{2\ell+1}\left(|\Phi_{\ell 0 p}|^2 + \sum_{j=J_0}^{J}\sum_{j'=J'_0}^{J'} |\Psi^{jj'}_{\ell 0 p}|^2\right) = 1, \forall \ell, p.$$

Scale-discretised wavelets on the ball

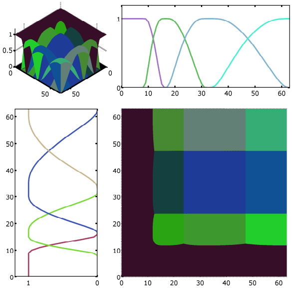

Figure: Tiling of Fourier-Laguerre space.

- Leistedt & JDM (2012)
  Exact wavelets on the ball
  FLAGLET code
- Define translation and convolution operator on the radial line.
- Dilation performed in harmonic space.
- The scale-discretised wavelet $\Psi \in \mathrm{L}^2(\mathrm{B}^3, \mathrm{d}^3\boldsymbol{r})$ is defined in harmonic space:

$$\Psi^{jj'}_{\ell m p} \equiv \sqrt{\frac{2\ell+1}{4\pi}}\, \kappa_\lambda\left(\frac{\ell}{\lambda^j}\right) \kappa_\nu\left(\frac{p}{\nu^{j'}}\right) \delta_{m0}\,.$$

- Construct wavelets to satisfy a resolution of the identity:

$$\frac{4\pi}{2\ell+1}\left(|\Phi_{\ell 0 p}|^2 + \sum_{j=J_0}^{J} \sum_{j'=J'_0}^{J'} |\Psi^{jj'}_{\ell 0 p}|^2 \right) = 1, \forall \ell, p.$$

Scale-discretised wavelets on the ball

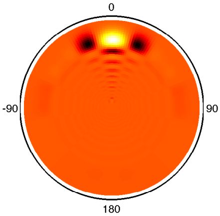

(a) $(j, j') = (4, 5)$

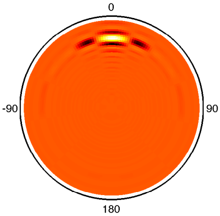

(b) $(j, j') = (4, 6)$

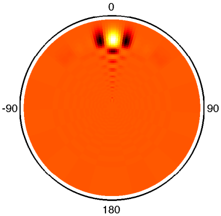

(c) $(j, j') = (5, 5)$

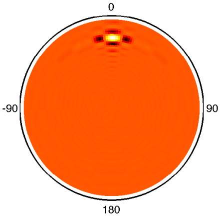

(d) $(j, j') = (5, 6)$

Figure: Scale-discretised wavelets on the ball.

Scale-discretised wavelets on the ball

- The scale-discretised wavelet transform is given by the usual projection onto each wavelet:

$$\boxed{W^{\Psi^{jj'}}(\boldsymbol{r}) \equiv (f \star \Psi^{jj'})(\boldsymbol{r}) = \langle f | \mathcal{T}_r \mathcal{R}_\omega \Psi^{jj'} \rangle \,.}$$

- The original function may be recovered exactly in practice from the wavelet (and scaling) coefficients:

$$\boxed{f(\boldsymbol{r}) \;=\; \int_{B^3} \mathrm{d}^3\boldsymbol{r}' \, W^{\Phi}(\boldsymbol{r}')(\mathcal{T}_r \mathcal{R}_\omega \Phi)(\boldsymbol{r}') + \sum_{j=J_0}^{J} \sum_{j'=J'_0}^{J'} \int_{B^3} \mathrm{d}^3\boldsymbol{r}' \, W^{\Psi^{jj'}}(\boldsymbol{r}')(\mathcal{T}_r \mathcal{R}_\omega \Psi^{jj'})(\boldsymbol{r}') \,.}$$

Scale-discretised wavelet denoising on the ball

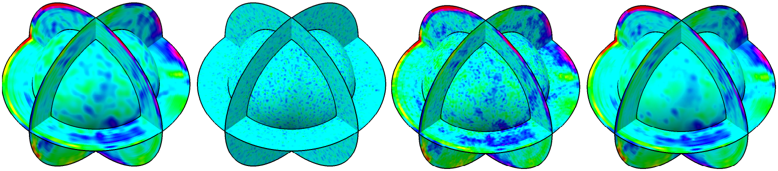

(a) Ground truth (b) Noise (c) Noisy (SNR=5dB) (d) Denoised (SNR=17dB)

Figure: Denoising of a seismological Earth model.

Scale-discretised wavelet denoising on the ball

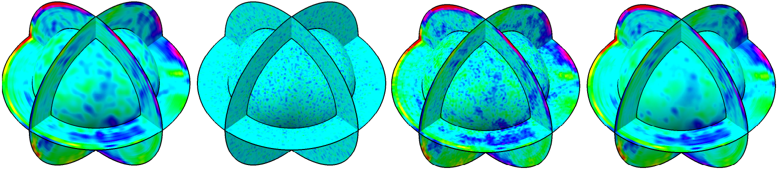

(a) Ground truth (b) Noise (c) Noisy (SNR=5dB) (d) Denoised (SNR=17dB)

Figure: Denoising of a seismological Earth model.

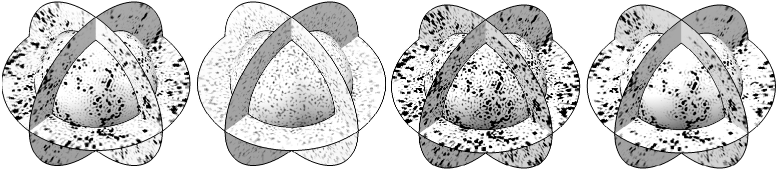

(a) Ground truth (b) Noise (c) Noisy (SNR=5dB) (d) Denoised (SNR=11dB)

Figure: Denoising of an N-body simulation.

Codes for scale-discretised wavelet on the ball

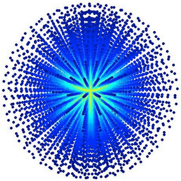

FLAG code
Exact wavelets on the ball
Leistedt & JDM (2012)

- C, Matlab, IDL, Java
- Exact Fourier-LAGuerre transform on the ball

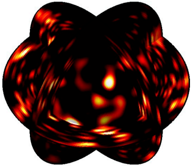

FLAGLET code
Exact wavelets on the ball
Leistedt & JDM (2012)

- C, Matlab, IDL, Java
- Exact (Fourier-LAGuerre) wavelets on the ball – coined *flaglets*!

All codes available from: `http://www.jasonmcewen.org/`

Outline

Compressive/compressed sensing/sampling (CS)

- **"Nothing short of revolutionary."**
  – National Science Foundation
- Developed by Emmanuel Candes and David Donoho (and others)
- Awards for Emmanuel Candes:
  - James H. Wilkinson Prize in 2005
  - Vasil A. Popov Prize in 2006 Alan T. Waterman Award in 2006
    – National Science Foundation's highest honour
  - George Polya Prize in 2010
  - ICIAM Collatz Prize in 2011

Compressive/compressed sensing/sampling (CS)

- **"Nothing short of revolutionary."**
  – National Science Foundation
- Developed by Emmanuel Candes and David Donoho (and others)
- Awards for Emmanuel Candes:
  - James H. Wilkinson Prize in 2005
  - Vasil A. Popov Prize in 2006 Alan T. Waterman Award in 2006
    – National Science Foundation's highest honour
  - George Polya Prize in 2010
  - ICIAM Collatz Prize in 2011

(a) Emmanuel Candes

(b) David Donoho

Compressive sensing

- Next evolution of wavelet analysis – wavelets are a key ingredient.
- The mystery of JPEG compression (discrete cosine transform; wavelet transform).
- Move compression to the acquisition stage $\rightarrow$ Compressive Sensing.

Compressive sensing

- Next evolution of wavelet analysis – wavelets are a key ingredient.
- The mystery of JPEG compression (discrete cosine transform; wavelet transform).
- Move compression to the acquisition stage $\longrightarrow$ Compressive Sensing.

Compressive sensing

- Next evolution of wavelet analysis – wavelets are a key ingredient.
- The mystery of JPEG compression (discrete cosine transform; wavelet transform).
- Move compression to the acquisition stage $\rightarrow$ Compressive Sensing.

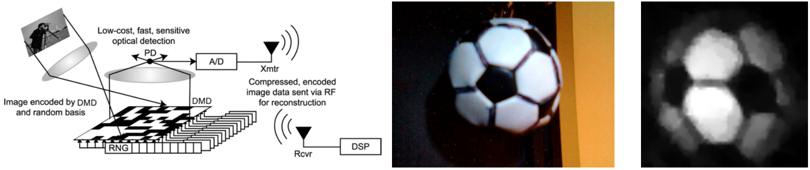

(a) Architecture (b) Scene (c) Recov. (20% meas.)

Figure: Single pixel camera

Introduction to the theory of compressive sensing

- Linear operator (linear algebra) representation of wavelet decomposition:

$$x(t) = \sum_i \alpha_i \Psi_i(t) \quad \rightarrow \quad \boldsymbol{x} = \sum_i \Psi_i \alpha_i = \begin{pmatrix} | \\ \Psi_0 \\ | \end{pmatrix} \alpha_0 + \begin{pmatrix} | \\ \Psi_1 \\ | \end{pmatrix} \alpha_1 + \cdots \quad \rightarrow \quad \boldsymbol{x} = \Psi \boldsymbol{\alpha}$$

- Linear operator (linear algebra) representation of measurement:

$$y_i = \langle x, \Phi_j \rangle \quad \rightarrow \quad \boldsymbol{y} = \begin{pmatrix} - \Phi_0 - \\ - \Phi_1 - \\ \vdots \end{pmatrix} \boldsymbol{x} \quad \rightarrow \quad \boldsymbol{y} = \Phi \boldsymbol{x}$$

- Putting it together: $\boldsymbol{y} = \Phi \boldsymbol{x} = \Phi \Psi \boldsymbol{\alpha}$

Introduction to the theory of compressive sensing

- Linear operator (linear algebra) representation of wavelet decomposition:

$$x(t) = \sum_i \alpha_i \Psi_i(t) \quad \rightarrow \quad \boldsymbol{x} = \sum_i \Psi_i \alpha_i = \begin{pmatrix} | \\ \Psi_0 \\ | \end{pmatrix} \alpha_0 + \begin{pmatrix} | \\ \Psi_1 \\ | \end{pmatrix} \alpha_1 + \cdots \quad \rightarrow \quad \boldsymbol{x} = \Psi \boldsymbol{\alpha}$$

- Linear operator (linear algebra) representation of measurement:

$$y_i = \langle x, \Phi_j \rangle \quad \rightarrow \quad \boldsymbol{y} = \begin{pmatrix} - & \Phi_0 & - \\ - & \Phi_1 & - \\ & \vdots & \end{pmatrix} \boldsymbol{x} \quad \rightarrow \quad \boldsymbol{y} = \Phi \boldsymbol{x}$$

- Putting it together: $\boldsymbol{y} = \Phi \boldsymbol{x} = \Phi \Psi \boldsymbol{\alpha}$

Introduction to the theory of compressive sensing

- Linear operator (linear algebra) representation of wavelet decomposition:

$$x(t) = \sum_i \alpha_i \Psi_i(t) \quad \rightarrow \quad \boldsymbol{x} = \sum_i \Psi_i \alpha_i = \begin{pmatrix} | \\ \Psi_0 \\ | \end{pmatrix} \alpha_0 + \begin{pmatrix} | \\ \Psi_1 \\ | \end{pmatrix} \alpha_1 + \cdots \quad \rightarrow \quad \boldsymbol{x} = \Psi \boldsymbol{\alpha}$$

- Linear operator (linear algebra) representation of measurement:

$$y_i = \langle x, \Phi_j \rangle \quad \rightarrow \quad \boldsymbol{y} = \begin{pmatrix} - & \Phi_0 & - \\ - & \Phi_1 & - \\ & \vdots & \end{pmatrix} \boldsymbol{x} \quad \rightarrow \quad \boldsymbol{y} = \Phi \boldsymbol{x}$$

- Putting it together: $\boldsymbol{y} = \Phi \boldsymbol{x} = \Phi \Psi \boldsymbol{\alpha}$

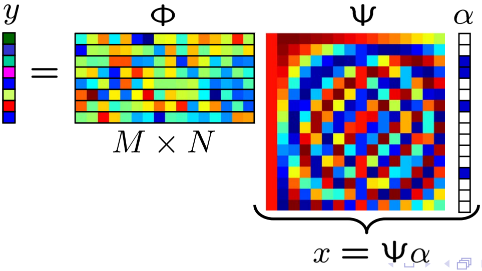

Introduction to the theory of compressive sensing

- Ill-posed inverse problem:

$$y = \Phi x + n = \Phi \Psi \alpha + n .$$

- Solve by imposing a regularising prior that the signal to be recovered is sparse in Ψ, *i.e.* solve the following ℓ_0 optimisation problem:

$$\alpha^\star = \arg\min_{\alpha} \|\alpha\|_0 \ \text{such that} \ \|y - \Phi\Psi\alpha\|_2 \leq \epsilon ,$$

where the signal is synthesising by $x^\star = \Psi \alpha^\star$.

- Recall norms given by

$$\|\alpha\|_0 = \text{no. non-zero elements} \qquad \|\alpha\|_1 = \sum_i |\alpha_i| \qquad \|\alpha\|_2 = \Big(\sum_i |\alpha_i|^2\Big)^{1/2}$$

- Solving this problem is difficult (combinatorial).
- Instead, solve the ℓ_1 optimisation problem (convex):

$$\alpha^\star = \arg\min_{\alpha} \|\alpha\|_1 \ \text{such that} \ \|y - \Phi\Psi\alpha\|_2 \leq \epsilon .$$

- The solutions of the ℓ_0 and ℓ_1 problems are often the same.

Introduction to the theory of compressive sensing

- Ill-posed inverse problem:

$$\boldsymbol{y} = \Phi \boldsymbol{x} + \boldsymbol{n} = \Phi \Psi \boldsymbol{\alpha} + \boldsymbol{n}.$$

- Solve by imposing a regularising prior that the signal to be recovered is sparse in Ψ, *i.e.* solve the following ℓ_0 optimisation problem:

$$\boldsymbol{\alpha}^\star = \underset{\boldsymbol{\alpha}}{\arg\min} \|\alpha\|_0 \;\text{ such that }\; \|\boldsymbol{y} - \Phi\Psi\boldsymbol{\alpha}\|_2 \leq \epsilon \,,$$

  where the signal is synthesising by $\boldsymbol{x}^\star = \Psi \boldsymbol{\alpha}^\star$.

- Recall norms given by

$$\|\alpha\|_0 = \text{no. non-zero elements} \qquad \|\alpha\|_1 = \sum_i |\alpha_i| \qquad \|\alpha\|_2 = \Big(\sum_i |\alpha_i|^2\Big)^{1/2}$$

- Solving this problem is difficult (combinatorial).
- Instead, solve the ℓ_1 optimisation problem (convex):

$$\boldsymbol{\alpha}^\star = \underset{\boldsymbol{\alpha}}{\arg\min} \|\alpha\|_1 \;\text{ such that }\; \|\boldsymbol{y} - \Phi\Psi\boldsymbol{\alpha}\|_2 \leq \epsilon \,.$$

- The solutions of the ℓ_0 and ℓ_1 problems are often the same.

Introduction to the theory of compressive sensing

- Ill-posed inverse problem:
$$\boldsymbol{y} = \Phi \boldsymbol{x} + \boldsymbol{n} = \Phi \Psi \boldsymbol{\alpha} + \boldsymbol{n} .$$

- Solve by imposing a regularising prior that the signal to be recovered is sparse in Ψ, *i.e.* solve the following ℓ_0 optimisation problem:
$$\boldsymbol{\alpha}^\star = \arg\min_{\boldsymbol{\alpha}} \|\alpha\|_0 \ \text{ such that } \ \|\boldsymbol{y} - \Phi\Psi\boldsymbol{\alpha}\|_2 \leq \epsilon ,$$
where the signal is synthesising by $\boldsymbol{x}^\star = \Psi \boldsymbol{\alpha}^\star$.

- Recall norms given by
$$\|\alpha\|_0 = \text{no. non-zero elements} \qquad \|\alpha\|_1 = \sum_i |\alpha_i| \qquad \|\alpha\|_2 = \Big(\sum_i |\alpha_i|^2\Big)^{1/2}$$

- Solving this problem is difficult (combinatorial).

- Instead, solve the ℓ_1 optimisation problem (convex):
$$\boldsymbol{\alpha}^\star = \arg\min_{\boldsymbol{\alpha}} \|\alpha\|_1 \ \text{ such that } \ \|\boldsymbol{y} - \Phi\Psi\boldsymbol{\alpha}\|_2 \leq \epsilon .$$

- The solutions of the ℓ_0 and ℓ_1 problems are often the same.

Introduction to the theory of compressive sensing

- Ill-posed inverse problem:

$$\boldsymbol{y} = \Phi \boldsymbol{x} + \boldsymbol{n} = \Phi \Psi \boldsymbol{\alpha} + \boldsymbol{n} .$$

- Solve by imposing a regularising prior that the signal to be recovered is sparse in Ψ, *i.e.* solve the following ℓ_0 optimisation problem:

$$\boldsymbol{\alpha}^\star = \underset{\boldsymbol{\alpha}}{\arg\min} \|\alpha\|_0 \text{ such that } \|\boldsymbol{y} - \Phi \Psi \boldsymbol{\alpha}\|_2 \leq \epsilon \,,$$

  where the signal is synthesising by $\boldsymbol{x}^\star = \Psi \boldsymbol{\alpha}^\star$.

- Recall norms given by

$$\|\alpha\|_0 = \text{no. non-zero elements} \qquad \|\alpha\|_1 = \sum_i |\alpha_i| \qquad \|\alpha\|_2 = \Big(\sum_i |\alpha_i|^2\Big)^{1/2}$$

- Solving this problem is difficult (combinatorial).
- Instead, solve the ℓ_1 optimisation problem (convex):

$$\boldsymbol{\alpha}^\star = \underset{\boldsymbol{\alpha}}{\arg\min} \|\alpha\|_1 \text{ such that } \|\boldsymbol{y} - \Phi \Psi \boldsymbol{\alpha}\|_2 \leq \epsilon \,.$$

- The solutions of the ℓ_0 and ℓ_1 problems are often the same.

Introduction to the theory of compressive sensing

- Ill-posed inverse problem:

$$\boldsymbol{y} = \Phi \boldsymbol{x} + \boldsymbol{n} = \Phi \Psi \boldsymbol{\alpha} + \boldsymbol{n} .$$

- Solve by imposing a regularising prior that the signal to be recovered is sparse in Ψ, *i.e.* solve the following ℓ_0 optimisation problem:

$$\boldsymbol{\alpha}^\star = \arg\min_{\boldsymbol{\alpha}} \|\alpha\|_0 \text{ such that } \|\boldsymbol{y} - \Phi\Psi\boldsymbol{\alpha}\|_2 \leq \epsilon ,$$

  where the signal is synthesising by $\boldsymbol{x}^\star = \Psi \boldsymbol{\alpha}^\star$.

- Recall norms given by

$$\|\alpha\|_0 = \text{no. non-zero elements} \qquad \|\alpha\|_1 = \sum_i |\alpha_i| \qquad \|\alpha\|_2 = \Big(\sum_i |\alpha_i|^2\Big)^{1/2}$$

- Solving this problem is difficult (combinatorial).
- Instead, solve the ℓ_1 optimisation problem (convex):

$$\boldsymbol{\alpha}^\star = \arg\min_{\boldsymbol{\alpha}} \|\alpha\|_1 \text{ such that } \|\boldsymbol{y} - \Phi\Psi\boldsymbol{\alpha}\|_2 \leq \epsilon .$$

- The solutions of the ℓ_0 and ℓ_1 problems are often the same.

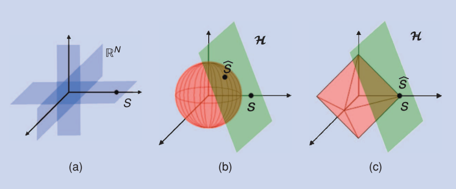

Introduction to the theory of compressive sensing

- In the absence of noise, compressed sensing is **exact!**
- Number of measurements required to achieve exact reconstruction is given by

$$M \geq c\mu^2 K \log N ,$$

where K is the sparsity and N the dimensionality.

- The coherence between the measurement and sparsity basis is given by

$$\mu = \sqrt{N} \max_{i,j} |\langle \Psi_i, \Phi_j \rangle| .$$

- Robust to noise.
- Many new developments (*e.g.* analysis vs synthesis, cosparsity, structured sparsity) and new applications.

Introduction to the theory of compressive sensing

- In the absence of noise, compressed sensing is **exact!**
- Number of measurements required to achieve exact reconstruction is given by

$$M \geq c\mu^2 K \log N \, ,$$

where K is the sparsity and N the dimensionality.

- The coherence between the measurement and sparsity basis is given by

$$\mu = \sqrt{N} \max_{i,j} |\langle \Psi_i, \Phi_j \rangle| \, .$$

- Robust to noise.
- Many new developments (*e.g.* analysis vs synthesis, cosparsity, structured sparsity) and new applications.

Introduction to the theory of compressive sensing

- In the absence of noise, compressed sensing is **exact!**
- Number of measurements required to achieve exact reconstruction is given by

$$M \geq c\mu^2 K \log N \,,$$

where K is the sparsity and N the dimensionality.

- The coherence between the measurement and sparsity basis is given by

$$\mu = \sqrt{N} \max_{i,j} |\langle \Psi_i, \Phi_j \rangle| \,.$$

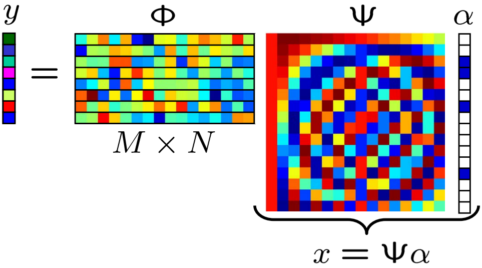

- Robust to noise.
- Many new developments (*e.g.* analysis vs synthesis, cosparsity, structured sparsity) and new applications.

Introduction to the theory of compressive sensing

- In the absence of noise, compressed sensing is **exact!**
- Number of measurements required to achieve exact reconstruction is given by

$$M \geq c\mu^2 K \log N \,,$$

where K is the sparsity and N the dimensionality.

- The coherence between the measurement and sparsity basis is given by

$$\mu = \sqrt{N} \max_{i,j} |\langle \Psi_i, \Phi_j \rangle| \,.$$

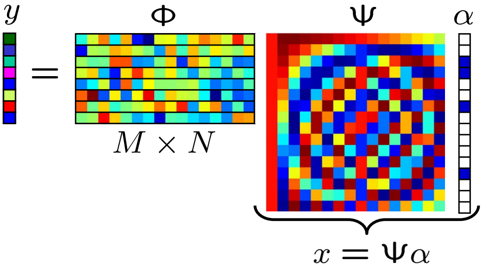

- Robust to noise.
- Many new developments (*e.g.* analysis vs synthesis, cosparsity, structured sparsity) and new applications.

Outline

Next-generation of radio interferometry rapidly approaching

- Square Kilometre Array (SKA) first observations planned for 2019.
- Many other pathfinder telescopes under construction, *e.g.* LOFAR, ASKAP, MeerKAT, MWA.
- New modelling and imaging techniques required to ensure the next-generation of interferometric telescopes reach their full potential.

Figure: Artist impression of SKA dishes. [Credit: SKA Organisation]

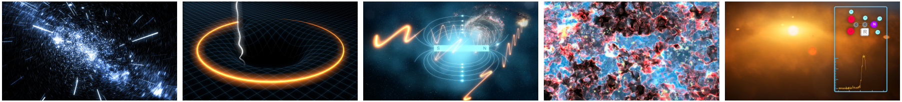

(a) Dark-energy (b) GR (c) Cosmic magnetism (d) EoR (e) Exoplanets

Figure: SKA science goals. [Credit: SKA Organisation]

Radio interferometry

- The complex visibility measured by an interferometer is given by

$$y(\boldsymbol{u}, w) = \int_{D^2} A(\boldsymbol{l})\, x_{\rm p}(\boldsymbol{l})\, \mathrm{e}^{-\mathrm{i}2\pi[\boldsymbol{u}\cdot\boldsymbol{l} + w\,(n(\boldsymbol{l})-1)]}\, \frac{\mathrm{d}^2\boldsymbol{l}}{n(\boldsymbol{l})}$$
$$= \int_{D^2} A(\boldsymbol{l})\, x_{\rm p}(\boldsymbol{l})\, C(\|\boldsymbol{l}\|_2)\, \mathrm{e}^{-\mathrm{i}2\pi\boldsymbol{u}\cdot\boldsymbol{l}}\, \frac{\mathrm{d}^2\boldsymbol{l}}{n(\boldsymbol{l})}\ ,$$

where $\boldsymbol{l} = (l, m)$, $\|\boldsymbol{l}\|^2 + n^2(\boldsymbol{l}) = 1$ and the w-component $C(\|\boldsymbol{l}\|_2)$ is given by

$$C(\|\boldsymbol{l}\|_2) \equiv \mathrm{e}^{\mathrm{i}2\pi w\left(1-\sqrt{1-\|\boldsymbol{l}\|^2}\right)}\ .$$

- Various assumptions are often made regarding the size of the field-of-view (FoV):
  - Small-field with $\|\boldsymbol{l}\|^2\, w \ll 1 \quad \Rightarrow \quad C(\|\boldsymbol{l}\|_2) \simeq 1$
  - Small-field with $\|\boldsymbol{l}\|^4\, w \ll 1 \quad \Rightarrow \quad C(\|\boldsymbol{l}\|_2) \simeq \mathrm{e}^{\mathrm{i}\pi w\|\boldsymbol{l}\|^2}$
  - Wide-field $\quad \Rightarrow \quad C(\|\boldsymbol{l}\|_2) = \mathrm{e}^{\mathrm{i}2\pi w\left(1-\sqrt{1-\|\boldsymbol{l}\|^2}\right)}$

- Interferometric imaging: recover an image from noisy and incomplete Fourier measurements.

Radio interferometric inverse problem

- Consider the resulting ill-posed inverse problem posed in the discrete setting:

$$\boldsymbol{y} = \Phi \boldsymbol{x} + \boldsymbol{n} \ ,$$

  with:
  - incomplete Fourier measurements taken by the interferometer $\boldsymbol{y}$;
  - linear measurement operator Φ;
  - underlying image $\boldsymbol{x}$;
  - noise $\boldsymbol{n}$.

- Measurement operator $\Phi = \mathbf{M}\,\mathbf{F}\,\mathbf{C}\,\mathbf{A}$ incorporates:
  - primary beam $\mathbf{A}$ of the telescope;
  - w-component modulation $\mathbf{C}$ (responsible for the spread spectrum phenomenon);
  - Fourier transform $\mathbf{F}$;
  - masking $\mathbf{M}$ which encodes the incomplete measurements taken by the interferometer.

Interferometric imaging with compressed sensing

- Solve by applying a prior on sparsity of the signal in a sparsifying basis Ψ or in the magnitude of its gradient.
- Recover image by solving:
  - Basis Pursuit denoising problem

$$\boldsymbol{\alpha}^\star = \underset{\boldsymbol{\alpha}}{\arg\min} \|\alpha\|_1 \text{ such that } \|\boldsymbol{y} - \Phi\Psi\boldsymbol{\alpha}\|_2 \leq \epsilon \,,$$

    where the image is synthesising by $\boldsymbol{x}^\star = \Psi\boldsymbol{\alpha}^\star$;
  - Total Variation (TV) denoising problem

$$\boldsymbol{x}^\star = \underset{\boldsymbol{x}}{\arg\min} \|\boldsymbol{x}\|_{\mathrm{TV}} \text{ such that } \|\boldsymbol{y} - \Phi\boldsymbol{x}\|_2 \leq \epsilon \,.$$

- ℓ_1-norm $\|\cdot\|_1$ is given by the sum of the absolute values of the signal.
- TV norm $\|\cdot\|_{\mathrm{TV}}$ is given by the ℓ_1-norm of the gradient of the signal.
- Tolerance ϵ is related to an estimate of the noise variance.

SARA for RI imaging

- Sparsity averaging reweighted analysis (SARA) for RI imaging (Carrillo, JDM & Wiaux 2012)
- Consider a dictionary composed of a concatenation of orthonormal bases, i.e.

$$\boxed{\Psi = \frac{1}{\sqrt{q}}[\Psi_1, \Psi_2, \ldots, \Psi_q],}$$

  thus $\Psi \in \mathbb{R}^{N \times D}$ with $D = qN$.
- We consider the following bases:
  - Dirac, *i.e.* pixel basis
  - Haar wavelets (promotes gradient sparsity)
  - Daubechies wavelet bases two to eight.

  $\Rightarrow$ concatenation of 9 bases
- Promote average sparsity by solving the reweighted ℓ_1 analysis problem:

$$\boxed{\min_{\bar{x} \in \mathbb{R}^N} \|W\Psi^T\bar{x}\|_1 \quad \text{subject to} \quad \|y - \Phi\bar{x}\|_2 \leq \epsilon \quad \text{and} \quad \bar{x} \geq 0\,,}$$

  where $W \in \mathbb{R}^{D \times D}$ is a diagonal matrix with positive weights.
- Solve a sequence of reweighted ℓ_1 problems using the solution of the previous problem as the inverse weights $\rightarrow$ approximate the ℓ_0 problem.

SARA for RI imaging

- Sparsity averaging reweighted analysis (SARA) for RI imaging (Carrillo, JDM & Wiaux 2012)
- Consider a dictionary composed of a concatenation of orthonormal bases, i.e.

$$\boxed{\Psi = \frac{1}{\sqrt{q}} [\Psi_1, \Psi_2, \ldots, \Psi_q],}$$

  thus $\Psi \in \mathbb{R}^{N \times D}$ with $D = qN$.

- We consider the following bases:
  - Dirac, *i.e.* pixel basis
  - Haar wavelets (promotes gradient sparsity)
  - Daubechies wavelet bases two to eight.

  $\Rightarrow$ concatenation of 9 bases

- Promote average sparsity by solving the reweighted ℓ_1 analysis problem:

$$\boxed{\min_{\bar{\boldsymbol{x}} \in \mathbb{R}^N} \|W\Psi^T \bar{\boldsymbol{x}}\|_1 \quad \text{subject to} \quad \|\boldsymbol{y} - \Phi\bar{\boldsymbol{x}}\|_2 \leq \epsilon \quad \text{and} \quad \bar{\boldsymbol{x}} \geq 0\,,}$$

  where $W \in \mathbb{R}^{D \times D}$ is a diagonal matrix with positive weights.

- Solve a sequence of reweighted ℓ_1 problems using the solution of the previous problem as the inverse weights $\rightarrow$ approximate the ℓ_0 problem.

SARA for RI imaging

- Sparsity averaging reweighted analysis (SARA) for RI imaging (Carrillo, JDM & Wiaux 2012)
- Consider a dictionary composed of a concatenation of orthonormal bases, i.e.

$$\boxed{\Psi = \frac{1}{\sqrt{q}}[\Psi_1, \Psi_2, \dots, \Psi_q],}$$

  thus $\Psi \in \mathbb{R}^{N \times D}$ with $D = qN$.

- We consider the following bases:
  - Dirac, *i.e.* pixel basis
  - Haar wavelets (promotes gradient sparsity)
  - Daubechies wavelet bases two to eight.

  $\Rightarrow$ concatenation of 9 bases

- Promote average sparsity by solving the reweighted ℓ_1 analysis problem:

$$\boxed{\min_{\bar{\boldsymbol{x}} \in \mathbb{R}^N} \|W\Psi^T\bar{\boldsymbol{x}}\|_1 \quad \text{subject to} \quad \|\boldsymbol{y} - \Phi\bar{\boldsymbol{x}}\|_2 \leq \epsilon \quad \text{and} \quad \bar{\boldsymbol{x}} \geq 0\,,}$$

  where $W \in \mathbb{R}^{D \times D}$ is a diagonal matrix with positive weights.

- Solve a sequence of reweighted ℓ_1 problems using the solution of the previous problem as the inverse weights $\rightarrow$ approximate the ℓ_0 problem.

SARA for RI imaging

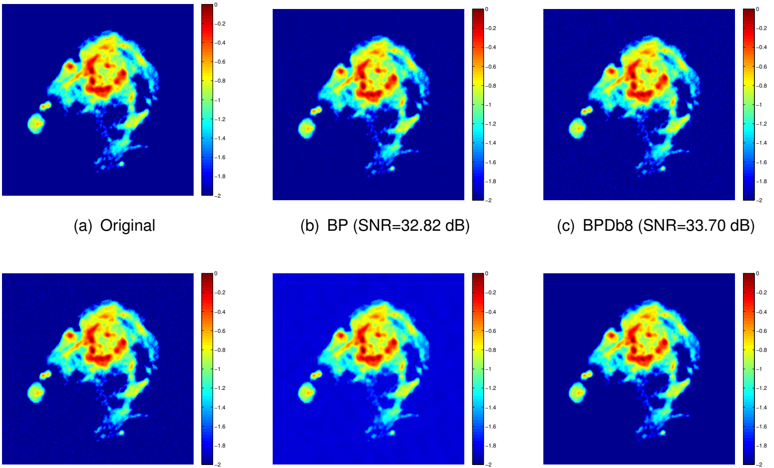

(a) Original

(b) BP (SNR=32.82 dB)

(c) BPDb8 (SNR=33.70 dB)

(d) IUWT (SNR=32.12 dB)

(e) TV (SNR=33.89 dB)

(f) SARA (SNR=38.43 dB)

Figure: Reconstruction example of M31 from 30% of visibilities.

SARA for RI imaging

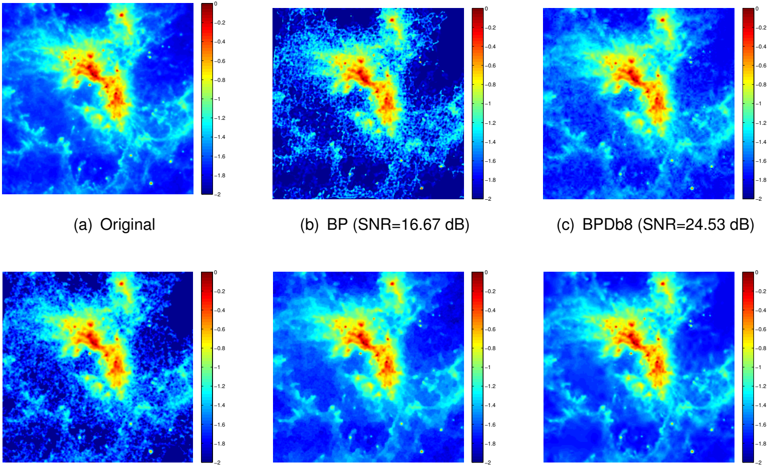

(a) Original (b) BP (SNR=16.67 dB) (c) BPDb8 (SNR=24.53 dB)

(d) IUWT (SNR=17.87 dB) (e) TV (SNR=26.47 d) (f) SARA (SNR=29.08 dB)

Figure: Reconstruction example of 30Dor from 30% of visibilities.

SARA for RI imaging

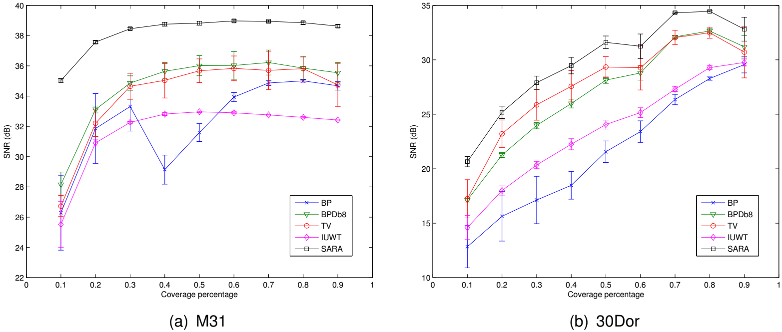

Figure: Reconstruction fidelity vs visibility coverage.

Future work

- Now that the effectiveness of these techniques has been demonstrated, it is of paramount importance to adapt them to realistic interferometric configurations.
- Continuous visibility coverage $\rightarrow$ incorporate a gridding operator in the measurement operator.
- Visibility coverage due to real interferometric observing strategies.
- Study the spread spectrum phenomenon due to wide fields of view in the presence of varying w (using the w-projection algorithm).
- Study the spread spectrum phenomenon in the presence of other direction dependent effects.
- Develop a new code in a low-level programming language (*e.g.* C) to go to big data-sets of real interferometric observations.

Future work

- Now that the effectiveness of these techniques has been demonstrated, it is of paramount importance to adapt them to realistic interferometric configurations.
- Continuous visibility coverage $\rightarrow$ incorporate a gridding operator in the measurement operator.
- Visibility coverage due to real interferometric observing strategies.
- Study the spread spectrum phenomenon due to wide fields of view in the presence of varying w (using the w-projection algorithm).
- Study the spread spectrum phenomenon in the presence of other direction dependent effects.
- Develop a new code in a low-level programming language (*e.g.* C) to go to big data-sets of real interferometric observations.

Outline